

Zubia-Aranburu Judith, Buruaga Lorea, Martin-Inaraja Myriam, Rodriguez Clara, Santos Silvia, Silván Unai, Eguizabal Cristina, and Zabala Alaitz. Towards tailored surface topography on electrospun wound dressings for exudate absorption. *Surface Innovations* 2024 12:3-4, 252-264

<https://doi.org/10.1680/jsuin.23.00044>

*Copyright © ICE Publishing, all rights reserved. This AAM is provided for your own personal use only. It may not be used for resale, reprinting, systematic distribution, emailing, or for any other commercial purpose without the permission of the publisher'*

**Accepted manuscript**

As a service to our authors and readers, we are putting peer-reviewed accepted manuscripts (AM) online, in the Ahead of Print section of each journal web page, shortly after acceptance.

**Disclaimer**

The AM is yet to be copyedited and formatted in journal house style but can still be read and referenced by quoting its unique reference number, the digital object identifier (DOI). Once the AM has been typeset, an ‘uncorrected proof’ PDF will replace the ‘accepted manuscript’ PDF. These formatted articles may still be corrected by the authors. During the Production process, errors may be discovered which could affect the content, and all legal disclaimers that apply to the journal relate to these versions also.

**Version of record**

The final edited article will be published in PDF and HTML and will contain all author corrections and is considered the version of record. Authors wishing to reference an article published Ahead of Print should quote its DOI. When an issue becomes available, queuing Ahead of Print articles will move to that issue’s Table of Contents. When the article is published in a journal issue, the full reference should be cited in addition to the DOI.

**Submitted:** 10 July 2023

**Published online in ‘accepted manuscript’ format:** 21 September 2023

**Manuscript title:** Towards tailored surface topography on electrospun wound dressings for maximised exudate absorption

**Authors:** Judith Zubia-Aranburu<sup>1</sup>, Lorea Buruaga<sup>1</sup>, Myriam Martin-Inaraja<sup>2,3</sup>, Clara Rodriguez<sup>2,3</sup>, Silvia Santos<sup>2,3</sup>, Unai Silván<sup>4,5</sup>, Cristina Eguizabal<sup>2,3</sup>, Alaitz Zabala<sup>1</sup>

**Affiliations:** <sup>1</sup>Mechanics and Industrial Production Department, Faculty of Engineering, Mondragon Unibertsitatea, Arrasate-Mondragón, Spain. <sup>2</sup>Research Unit, Basque Centre for Blood Transfusion and Human Tissues, Galdakao, Spain. <sup>3</sup>Cell Therapy, Stem Cells and Tissues Group, Biocruces Bizkaia Health Research Institute, Cell Therapy, Stem Cells and Tissues Group, Barakaldo, Spain. <sup>4</sup>BCMaterials, Basque Center for Materials, Applications and Nanostructures, UPV/EHU Science Park, Leioa, Spain. <sup>5</sup>Ikerbasque, Basque Foundation for Science, Bilbao, Spain.

**Corresponding author:** Alaitz Zabala, Mechanics and Industrial Production Department, Faculty of Engineering, Mondragon Unibertsitatea, 20500 Arrasate-Mondragón, Spain.

**E-mail:** azabalae@mondragon.edu

## Abstract

Because it can generate micro- to nanometre-scale fibres, electrospinning is widely used for fabricating wound dressings. Electrospun scaffolds with defined 3D patterns at the mat surface can be efficiently fabricated by textured collectors that transfer the topography during the manufacturing process. However, the efficacy of surface pattern transfer from the collector to the mat, the correlation between the topography and the absorption capability, and the effect of sterilisation on absorption have not yet been analysed. In this study, textured patterns were imprinted over PCL electrospun mats via textured collectors. The successful transferability of the patterns was quantified through height, hybrid and functional surface topography parameters. Additionally, EtO, H<sub>2</sub>O<sub>2</sub> and UV sterilisation methods were tested, of which only UV preserved the mat's morphological and functional integrity. Finally, fibroblasts were used to analyse the cytotoxicity and cellular response of the dressings, verifying their biocompatible nature. This study demonstrates that absorption capacity can be modulated by the surface texture of the wound dressing. The  $S_{dq}$  and  $S_{dr}$  parameters are identified as key surface characteristics for enhancing absorption capacity and yield an increase of up to 176.76% compared to the non-textured control, thus revealing the potential of surface functionalisation for increasing exudate absorption.

**Notation**

- $M_n$  Number Average Molecular Weight. The total number of molecules in a unit of mass.
- $S_a$  Arithmetical Mean Height. Absolute value of the difference in height of each point compared to the arithmetical mean of the surface.
- $S_q$  Root Mean Square Height. Standard deviation of the heights from the surface mean line.
- $S_{sk}$  Skewness. Third statistical moment, qualifying the symmetry of the height distribution.
- $S_{dr}$  Developed Interfacial Area Ratio. The percentage of additional surface area contributed by the texture as compared to an ideal plane.
- $S_{dq}$  Root Mean Square Gradient. Root mean square slope of the surface; it is a general measurement of the slopes which comprise the surface.
- $V_{mp}$  Peak Material Volume. Material volume enclosed in the 5% material ratio and normalised to unit sampling area.
- $V_{vv}$  Dale Void Volume. Void volume in the valley zone from 80% to 100% surface material ratio and normalised to the unit sampling area.

## 1. Introduction

Driven by rapid increases in life expectancy and the incidence of chronic diseases in recent years, the prevalence of chronic wounds is growing at an annual rate of 2% (1). This issue not only reduces the quality of life for patients and their relatives but also has a significant economic impact, with estimates of \$22 billion in wound care costs by 2024 worldwide (2). Given the medical burden at stake, there is an urgent need to mitigate this problem (3).

To facilitate effective wound healing, wound dressings that act as temporary matrices for cell seeding must be biocompatible, biodegradable and bioactive, allowing cell adhesion and proliferation as well as nutrient diffusion (4). Moreover, adequate mechanical properties, porosity, oxygen permeation and exudate absorption capabilities are of utmost importance for optimal scaffold performance (5), (6). Some of these characteristics, such as biocompatibility and biodegradability, are attained by using specific materials that meet the above requirements (7).

In this context, polycaprolactone (PCL) is one of the most widely used synthetic polymeric materials in the field of tissue engineering. It is characterised by its biocompatibility, porosity, thermal stability and low cost (8). Furthermore, due to its hydrophobic nature, PCL has a very slow biodegradability. In general terms, the versatility and manufacturability of PCL make it an ideal material for large-scale production and the advancement of surface modification (9).

Electrospinning is a focus of wound dressing manufacturing approaches due to its ability to generate scaffolds that mimic the extracellular matrix. Electrospinning can generate fibres

on micrometre to nanometre scales, producing dressings with high porosities and surface areas – features that are extremely relevant when addressing wound exudate. Wound exudate, a key product of the healing process, prevents the wound bed from drying out and eases cell, nutrient and growth factor migration. As the healing process progresses, the generation of exudate tends to decrease; in chronic wounds, however, the overproduction of exudate extends the inflammatory phase (10). Excess exudate leads to over-hydration of the wound, causing moisture leakage and skin weakening. Consequently, the extracellular matrix becomes badly damaged, thus hampering tissue regeneration and wound healing (11).

Since scaffolds are intended to be applied to patients' skin, sterility is essential (12). However, mats must remain unaltered after the sterilisation process, i.e., their morphological and functional integrity must be preserved (13). Because different materials may be diversely affected by the same sterilisation method, the sterilisation selection process can be challenging (14).

Several approaches can enhance a scaffold's properties, including its ability to absorb wound exudate. These strategies include the generation of porous fibres (by either modifying the relative humidity or using different solvent systems) (15), the enhancement of mat hydrophilicity (16) and the addition of drugs to core-shell fibres (17). Based on evidence obtained using previous strategies, exudate absorption could potentially be improved by increasing the developed surface area of the electrospun mat (18), which can be achieved by transferring the topography through tailored textured collectors. To date, some work has been carried out in the development of 3D printed collectors with tuned topographical features and

geometries (19), (20). For instance, Rogers et. al. (21) fabricated electrospun scaffolds over 3D printed collectors containing 3D directional cues shown to influence cell behaviour. Hosseini et. al. (22) produced 3D patterned scaffolds to tune fibre orientation and analyse the attachment of chondrocyte cells. Grgurić et. al. (23) demonstrated the feasibility of controlling cell attachment and differentiation through the geometry of the collector, making it possible to meet specific tissue requirements by adjusting the geometry of the scaffold. Finally, Zdraveva et. al. (24) studied the effects of different structural patterns on both the mechanical properties and cellular responses of the mats.

However, to the authors' knowledge, several aspects remain unknown in the field. The novelty of the present study is rooted in the investigation of the following points: (i) the efficacy of surface pattern transfer from the collector to the mat, (ii) the correlation (if any) between topography and absorption capability and (iii) the effect of sterilisation on absorption capability.

To that end, textured collectors were used to transfer different surface patterns onto electrospun mats that were then sterilised with EtO, H<sub>2</sub>O<sub>2</sub> and UV. After selecting UV as the optimal sterilisation technique, mat properties such as fibre diameter, wettability and absorption capability were quantified with the goal of analysing how the sterilisation procedure affected the performances and surface properties of the electrospun mats. Moreover, the absorption capability of electrospun mats with different surface textures was correlated to specific surface parameters, demonstrating a direct correlation between the developed surface and the root mean square gradient with the absorption capability. Finally, cell viability and



proliferation assays were performed to assess the compatibility of the textured mats with the biological environment.

This study achieves notable progress toward the development of functionalised electrospun wound dressings with an improved capacity for exudate absorption. This functionalisation serves as a crucial element in accelerating the healing of chronic wounds by addressing issues such as excessive hydration, moisture leakage and skin debilitation.

## 2. Materials and methods

### 2.1 Materials

The electrospinning setup was established using a Genvolt 73030 variable high voltage power supply (output voltage = 0–30 kV) (UK), NE-300 Just Infusion™ syringe pump (USA) and a static collector plate wrapped with aluminium foil. Ambient conditions were controlled inside a Series 5000 humidity and temperature controller with an M 5461 molecular sieve desiccant dehumidification system and an Electro-Tech Systems M 5482 humidification system by Electro-Tech Systems (USA).

Poly( $\epsilon$ -caprolactone) (PCL) ( $M_n = 80,000$  g/mol) and chloroform ( $\text{CHCl}_3$ ; density = 1.484 g/ml at 20°C, boiling point = 61–62°C) were purchased from Sigma-Aldrich (USA). Hanks' Balanced Salt Solution (HBSS) was purchased from Thermo Fisher Scientific Inc. (USA).

For the fabrication of the electrospun mats with different textures, five embossed stainless steel plates from Acerinox (Spain) were used as controls (CC; Acerinox AISI 430 BA) and textured collectors (TC1, TC2, TC3 and TC4; Acerinox AISI 304 Emboss). The surface

morphologies and parameters of the plates are shown in Table 1.

## 2.2 *Electrospun mat fabrication*

The mats were prepared by electrospinning the 10% w/w PCL solution at a flow rate of 1 mL/h at a constant voltage of 10.5 kV, keeping a distance of 18 cm between the needle tip and the collector. To obtain a solution of 10% w/w, 10 g of PCL were dissolved in 12.13 mL of chloroform at room temperature while stirring overnight. The process was carried out at controlled temperature and humidity conditions of 21.5°C and 44.1%, respectively. Each of the mats was electrospun for 2 h.

The meshes were fabricated and detached from the collectors and then manually die-cut into 10 mm-diameter discs using a 10 mm-diameter manual punch (purchased from Kayser GmbH, Germany).

## 2.3 *Sterilisation*

All electrospun mats used in this study were sterilised using three different sterilisation methods under the following protocols: (i) with UV for 4 min at room temperature (CL-1000 Ultraviolet Crosslinker, UVP), (ii) with ethylene oxide (Steri-Vac 5XL, 3M) for 55 min at low temperature, without exceeding 60°C and (iii) with hydrogen peroxide (V-PRO1, STERIS) for 55 min at low temperature, without exceeding 60°C.

## 2.4 *Characterisation of the electrospun mats*

### 2.4.1 Surface topography

To characterise the texture transfer, areal surface texture characterisation of both the collectors

and the electrospun mats was carried out with a SensoFar S-NEOX optical profilometer using focus variation technology (25).

An acquisition area of 12,977.4 x 12,138.9  $\mu\text{m}$  was set using a 5x magnification objective (spatial sampling: 2.5  $\mu\text{m}$ , vertical resolution: 75 nm) to capture at least five representative motives of all the textures under study. SensoMap Premium 7.4 metrology software was used for data post-processing, which removed surface noise through a Gaussian filter ( $\lambda_s = 5 \mu\text{m}$ ; S-filter). The form was subtracted through a plane surface fitting (F-operator). For complete surface descriptions, surface topography parameters belonging to the height ( $S_a$  and  $S_{sk}$ ), hybrid ( $S_{dr}$  and  $S_{dq}$ ) and functional ( $V_{mp}$ , and  $V_{vv}$ ) families (S refers to surface; V refers to volume) were computed on the primary S-F surface following the ISO 25178 standard (26).

#### 2.4.2 Fibre diameter

The morphology of the fibres was analysed via a field emission scanning electron microscope (FEI Nova NanoSEM 450) at an accelerating voltage of 3 kV and low vacuum mode (50 Pa) to avoid coating the samples. The fibre diameter measurements were obtained by means of ImageJ software. The fibres to be measured were selected randomly. The statistical analysis of the results was performed via a one-way ANOVA parametric test. Data corresponding to fibre diameters was expressed as the mean  $\pm$  SD (standard deviation), considering statistical significance at a  $p$ -value  $< 0.05$ .

#### 2.4.3 Wettability

To characterise the hydrophobicity of the meshes, a 35  $\mu\text{L}$  HBSS droplet was deposited on

each of the mesh discs at room temperature, and an image was acquired. Using ImageJ software, contact angle measurements were obtained by measuring each side of the droplet five times and calculating the average and standard deviation. The statistical analysis of the results was performed via a one-way ANOVA parametric test. Data corresponding to contact angles was expressed as the mean  $\pm$  SD, considering statistical significance at a  $p$ -value  $< 0.05$ .

#### 2.4.4 Absorption

The absorption capacity of the mats was measured through gravimetry. First, dry electrospun mat discs of initial weight  $W_0$  were immersed in HBSS for 1 h, 24 h and 72 h. After the set time had elapsed, the excess water was removed from the meshes by placing each disc between two filter papers and applying a stainless steel plate of 21.73 g for 5 s. Each disc was immediately weighed in the XPR 205 Mettler Toledo microanalytical balance (USA) four times to obtain the final weight average,  $W_1$ . Between measurements, each disc was again immersed in the HBSS for 5 s, and the wiping process was repeated. The absorption values of each disc were computed using Equation 1:

$$Absorption = \frac{W_1 - W_0}{W_0} \times 100\% \quad (1)$$

A Student's t-test was used to compare the absorption values of the non-sterile mats with their UV-sterile counterparts, and a one-way ANOVA parametric test was used to analyse the statistical significance of the absorption values between the differently textured mats. Data was represented as the mean  $\pm$  SD, considering statistical significance at a  $p$ -value  $< 0.05$ .

### *2.5 Culture of human primary dermal fibroblast cells with electrospun mats*

Human foreskin fibroblast (HFF-1; ATCC company) cells were cultured on cell culture 24-well suspension plates (Sarstedt, 83.3922500) with each type of disk-shaped mat for 24 h, 48 h and 72 h. Before adding the cells, the mats were attached to a 13 mm-diameter coverslip with SYLGARD™ 184 Silicone Elastomer Kit (Dow corning, 1673921). A total of 50,000 cells were seeded in each well in medium IMDM (1X) (Gibco, 12440-053) supplemented with 10% FBS (Invitrogen, 10270-106), 1% penicillin/streptomycin (Invitrogen, 15140-122) and 1% glutMAX (Gibco, 35050-061). Cells were incubated in 5% CO<sub>2</sub> on air at 37°C.

### *2.6 Immunofluorescence analysis. Cell viability and proliferation assays*

Cultured HFF-1 cells that were seeded on the electrospun mats were processed for immunofluorescence after 24 h, 48 h and 72 h in culture for both viability and proliferation assays. For the cell viability assay, the LIVE/DEAD Viability/Cytotoxicity Kit (Invitrogen, L3224) was used as described by the manufacturer, and cells were counterstained with NucBlue™ Live ReadyProbes™ (Hoechst 33342) (Invitrogen, R37605). For the proliferation analysis, cells were washed with PBS and fixed with 4% PFA at room temperature for 20 min. After fixation, cells were permeabilised with 0.1% (v/v) Triton X-100 in PBS for 7 min. Next, cells were washed with PBS and incubated for 2 h at room temperature with the primary antibody Ki67 (Fisher, 12683697) 1:200 in PBS. Thereafter, cells were washed with PBS three times and incubated for 1 h at room temperature with secondary antibody Alexa Fluor 488 donkey anti-rabbit (Invitrogen, A21206) 1:200 in PBS, followed by 30 min at room

temperature with ActinRed™ 555 ReadyProbes™ Reagent (Rhodamine phalloidin) (Invitrogen, R37112). Following 5 min of washing with PBS, cells were counterstained with NucBlue™ Live ReadyProbes™ (Hoechst 33342) (Invitrogen, R37605) and checked with the microscope.

### *2.7 Imaging, quantification and statistical analysis*

Immunofluorescence images were obtained using a DMI8 microscope (Leica) with a 20x/0.70 objective. Cultured HFF-1 (N = 3) was quantified by counting the cells in 10 different images (3000 mm<sup>2</sup>). The total number of positive cells per area counted in each condition is shown in Table 2. Image analysis and cell quantification were performed using Image J. GraphPad Prism 7.0a (GraphPad software Inc.) was used to create graphs and to conduct statistical analysis using the Student's t-test ( $p < 0.05$ ). Data is shown as the mean  $\pm$  SEM.

## **3. Results**

### *3.1 Topographical characterisation of collectors and electrospun mats*

Figure 1 shows the axonometric projections of the control and textured collector measurements, together with the corresponding mats that were electrospun on them. Figure 2 provides comparisons of the computed topographic parameters for each collector-electrospun mat pair for all the collector types under study.

As Figure 1 shows, the surface textures of the collectors were successfully transferred to the electrospun mats. This result is further verified via the skewness parameter ( $S_{sk}$ ), which exhibits a sign shift when the collector measurements are compared to the corresponding mat measurements (see Figure 2). This parameter indicates that the negative surface was transferred

to the mats, since a negative  $S_{sk}$  indicates a predominance of valleys, whereas a positive  $S_{sk}$  indicates a predominance of peaks. It should be noted that this sign shift is not observed in the control collector, since no texture was transferred in this case. Regarding the height parameter  $S_a$ , different trends are observed when comparing collector-mat pairs. In some instances, the mat value is larger than the value of the corresponding collector (CC, TC1). Others show similar values (TC2, TC3). TC4 yields a smaller value on the mat. These results indicate that in terms of depth, the transfer was not equal in all cases. In the case of TC4, it can be concluded that the texture transfer was less efficient than with the other collectors since the mean height of the mat is significantly smaller. The larger  $S_a$  of the mats corresponding to the CC and TC1 cases is associated with a combination of the height contributed by the fibres along with the waviness of the electrospun mat, which can be observed in Figure 1.

Regarding hybrid parameters ( $S_{dr}$ ,  $S_{dq}$ ), in all cases present, the mats display a significant increase in developed surface area ( $S_{dr}$ ) compared to their corresponding collectors, which is associated with the presence of surface fibres. Accordingly, the root mean square slope of the surface ( $S_{dq}$ ), which is a general measurement of the slopes that comprise the surface, is also larger for the mats. The functional parameters of the mats ( $V_{mp}$ ,  $V_{vv}$ ) also have higher values than those of the corresponding collectors, indicating that there is a greater volume of material on the peaks and in the valleys, respectively. An increased volume in the valleys is associated with an increased capacity to retain liquids.

### *3.2 Effect of sterilisation on electrospun mat integrity*

As the sterilisation procedure involves physical or chemical treatments that can compromise a

mat's topography and morphology as well as its optimised surface properties, the effects of different sterilisation techniques on the integrity of the electrospun mats were analysed. Figure 3 shows SEM images of the control (CC) and textured (TC1, TC2, TC3, TC4) electrospun mats without sterilisation and after the different sterilisation methods (EtO, H<sub>2</sub>O<sub>2</sub>, UV). All of the non-sterile mats display a fibrous structure. For the sterilised mats, even having considered techniques that cause less detrimental effects, some alterations can be observed depending on the method. EtO sterilisation completely damaged the mats, destroying the fibrous structures and converting the mats to non-porous, flat surfaces. In the case of H<sub>2</sub>O<sub>2</sub>, the same effect was observed, but only in two (TC3, TC4) of the five cases under analysis, which correspond to the textured collectors with the highest  $S_a$  values. Contrarily, UV sterilisation did not produce any changes in the fibrous structure of any of the mats. Indeed, the pores on the fibre surfaces could be observed after the UV sterilisation process. Based on the obtained results, the UV sterilisation method was selected for the following studies.

### *3.3 Effect of sterilisation on fibre diameters*

Fibre diameter is a parameter that should be considered when assessing electrospun mat absorption or cell attachment behaviour, since it determines the surface area of the fibres. Figure 4 shows the measured fibre diameters of the non-sterilised and UV-sterilised electrospun mats. Non-sterilised mat fibre diameters vary from one textured collector to another, although no correlation with the texture degree of the collector was found. Statistical analysis of the fibre diameters of non-sterilised mats revealed that there was no statistically significant difference between the diameters of fibres present in the non-textured control



collector (CC) and in textured collectors TC2 and TC4. In contrast, fibre diameters were significantly different ( $p < 0.05$ ) in TC1 and TC3. The greatest difference in fibre diameter with respect to the CC was found in the TC3 electrospun mat, with a maximum fibre diameter of 12.1  $\mu\text{m}$ . The smallest diameter corresponded to TC1, with a value of 4.9  $\mu\text{m}$ .

Regarding the effect of sterilisation on fibre diameter, different trends were encountered. For the non-textured control collector (CC), the diameter did not vary after sterilisation. Conversely, diameters did vary for the textured collectors. The diameter increased in some cases (TC1, TC4) and decreased in others (TC2, TC3), although differences were statistically significant only for TC3 and TC4.

### *3.4 Effect of sterilisation on hydrophobicity*

The hydrophobicity of the electrospun mats was characterised both in the non-sterilized and UV-sterilised samples (see Figure 5). No significant contact angle differences were observed between the sterile and non-sterile mats, regardless of the mat texture.

### *3.5 Effect of sterilisation and surface texture on absorption*

Figure 6 shows the absorption capability of the mats for the non-sterilised (see Figure 6a) and UV-sterilised (Figure 6b) samples. Overall, the same absorption values and trends were observed, indicating that UV sterilisation did not alter the absorption capability of the mats. Indeed, the t-test statistical analysis performed to identify statistically significant differences between each non-sterile mat and its UV-sterile counterpart revealed a significant difference ( $p < 0.05$ ) only for the TC4 mat at 1 h.

Absorption increased with immersion time in all the cases under study. The absorption capability differed between the different electrospun mats, with TC2 presenting the highest absorption, followed by TC4. These two mats presented a statistically significant difference ( $p < 0.05$ ) for absorption with respect to CC in the one-way ANOVA statistical test. Finally, TC3 and TC1 showed lower absorption values, similar to those of CC.

In terms of increased absorption of the textured mats with respect to the control, the TC2 and TC4 wound dressings increased by 176.76% and 161.55%, respectively, after 1 h of use; by 99.38% and 65.62%, respectively, after 1 day of use; and by 58.25% and 46.4%, respectively, after 3 days of use.

Accordingly, the present study shows that the absorption capability can be modulated by the mat surface texture. To identify any correlations between the topographic parameters and the absorption capability, all topographic parameters were normalised to the texture that yielded the highest absorption capability (TC2) and plotted in descending order on the X axis (see Figure 7).

Height and functional parameters did not show any trends that correlate with absorption. Conversely, both hybrid parameters ( $S_{dr}$ , and  $S_{dq}$ ) exhibited a correlation with absorption and are therefore identified as key topographic parameters for increasing absorption capability.

### 3.6 Cytotoxicity test

Figure 8 shows the percentages of cells that were alive and dead after the cytotoxicity test. Most cells appeared to be alive in the CC and TC4 collectors; TC2 showed the lowest percentages of living cells. Results were statistically significant for TC2 and TC4.

### 3.7 Cellular response

Figure 9 shows the cell proliferation in percentage at different culture times (24 h, 48 h, 72 h) for all textures under study. The statistical analysis reported no statistical differences between the groups. Accordingly, it can be concluded that the textures did not affect the behaviour of proliferating cells.

Although no statistically significant results were obtained, CC, TC3 and TC4 recorded the highest proliferation of fibroblasts. The lowest proliferation rates were recorded by TC1.

## 4. Discussion

Due to the characteristic excessive exudate production of chronic wounds, the absorption capacity of wound dressings is paramount. In this study, the effect of surface texture on the absorption capacity of PCL electrospun mats was analysed for the first time.

A cost-effective manufacturing process consisting of textured collectors that transfer a negative texture to the electrospun dressings was carried out. Although this process was previously introduced in the literature for cell behaviour enhancement purposes (21) (22) (23), the transferability analysis relied on qualitative visual inspection. In this study, different surface patterns were analysed for absorption maximisation, and the texture transferability of the electrospinning process was quantified using 3D areal topographical parameters. All the collector patterns under study were successfully transferred to the PCL mats, as indicated by sign shifts in the skewness parameters ( $S_{sk}$ ) between the collector and mat measurements; this result indicates the shift in predominance from peaks to valleys or vice versa. The functional

void volume ( $V_v$ ) parameter increased for all the textured surfaces compared to the non-textured control, indicating an increased capacity to retain liquids. Regarding transfer efficiency, the height  $S_a$  parameter showed different trends for different texture types, indicating that transferability varied among the different patterns.

Sterilisation is a crucial step prior to the use of the wound dressings; however, this process can modify wound dressing characteristics and is frequently an overlooked aspect. First, the effect of UV, EtO and  $H_2O_2$  sterilisation techniques on textured and non-textured mat integrity was analysed. No differences were observed between the textured and non-textured samples. SEM images revealed changes in the mat integrity of all samples sterilised with EtO and some samples sterilised with  $H_2O_2$ . None of the mats sterilised with UV radiation underwent topographical nor morphological changes. These results are consistent with those obtained by Ghobeira et. al. (27), who analysed the EtO,  $H_2O_2$  and UV sterilization techniques in conventional (non-textured) PCL electrospun mats. The authors concluded that EtO tends to increase hydrophobicity and produce changes in geometry, while the thermo-oxidative reactions associated with the  $H_2O_2$  method modify the electrospun mat architecture. Conversely, due to its non-chemical nature, the UV process did not cause any modifications. The present study analysed for the first time the effect of the sterilisation technique on textured PCL wound dressings, concluding that the effect resembles that observed on non-textured collectors. UV radiation proved to be the only feasible option for the sterilisation of the textured mats and was thus selected for further analyses of the effects of UV sterilisation on fibre diameter, hydrophobicity and absorption capacity.

Electrospun mats presented scatter on fibre diameters with values in the range of 4.9–12.1  $\mu\text{m}$ ; no trend was observed between the non-sterilised and UV-sterilised samples. Rogers et. al. (21) analysed the fibre diameter distribution on patterned mats, concluding that the fibre diameter can vary up to 55% between fibres located in peak or valley regions of the pattern. The random location measurements carried out in the present study could therefore be a possible source of the encountered diameter scatter. To achieve a consistent comparison between fibre diameters before and after sterilisation, the positions selected for measurement must be carefully selected and controlled in future studies.

Regarding the wettability of the dressings, no significant differences were encountered between the sterile and non-sterile mats, which is consistent with previous studies performed on non-textured PCL mats (14) (27). The differences between the textured and non-textured samples were not significant, suggesting that UV sterilisation does not produce any changes in the chemical surface compositions of the non-textured and textured dressings.

The absorption capacities of the electrospun mats remained unaltered after UV sterilisation for all textured and non-textured wound dressings. Compared to the non-textured control mats, two of the textured dressings, TC2 and TC4, yielded statistically significant absorption capacity increases of 176.76% and 161.55%, respectively, after 1 h of immersion, and 58.25% and 46.4%, respectively, after 3 days of immersion. A correlation study revealed that the absorption capacity correlates directly with the hybrid 3D areal topographic parameters  $S_{dr}$  and  $S_{dq}$ , which represent the developed surface area and mean slope of the surface, respectively. In this study, the relationship between surface topography and absorption

capability of PCL electrospun mats was established for the first time. The findings reveal the potential of surface functionalisation for exudate absorption optimisation and sets the quantitative bases for the design of new absorption maximisation functionalised wound dressings.

Finally, cytotoxicity and cell proliferation assays were performed to analyse and quantify the biocompatibility of the textured wound dressings. Although statistically significant differences were encountered on the live cell counts, the survival rates of all the samples were greater than 80%; therefore, all samples are considered acceptable. The cellular response of cultured HHF-1 cells showed no statistically significant differences between the different surface patterns. According to Metavarayuth et. al. (28), the cell response of isotropic pattern surfaces is often inconsistent, and in-depth analysis is difficult. Recent studies note that patterns that increase cell adhesion are similar in size to cells, so the cells can spread across the entire patterned surface (29). The scale of the textures used in the present study may therefore explain why textural effects on cell response were not observed. This finding is consistent with previous studies of textured collectors with similar or larger scales in which texture had no effect on cellular response (24). Additionally, the scatter of fibre diameters may offer another possible reason for the observed inconsistent cellular behaviour. Chen et al. (30) analysed the relationship between electrospun PCL mat fibre diameter values and NIH 3T3 fibroblast adhesion and growth kinetics, concluding that “the uniformness of fibre diameters may play an important role in modulating cellular attachment and proliferation in electrospun tissue engineering scaffolds”.

In the present work, the effect of wound dressing surface textures on wound exudate absorption was analysed and quantified for the first time. Electrospun wound dressings were functionalised by efficiently incorporating tailored surface textures into the dressings during the manufacturing process. Sterilisation via UV radiation maintained mat morphologies and properties. Moreover, surface textures increased the wound dressing capacity for wound exudate absorption by up to 176.76%. The biocompatibility of the mats was preserved, guaranteeing cellular activity and proliferation. Lastly, surface topography parameters that quantify surface texture transfer and directly influence exudate absorption were identified, presenting themselves as promising tools for future developments.

## 5. Conclusions

This study reported the development of textured electrospun PCL wound dressings for increased absorption of wound exudate as a way of improving the treatment of increasingly common chronic wounds. PCL was selected due to its biocompatibility, long biodegradability and suitability with electrospinning. The efficacy of texture transfer, the correlation between texture and absorption, the effect of sterilisation on functionality and the cellular viability were analysed. The following conclusions were drawn:

- Successful surface pattern transfer from the collector to the mat was achieved, numerically verified and quantified through 3D areal topographical parameters. In a comparison of collector and mat parameters, the mats displayed a shift in the skewness parameter ( $S_{sk}$ ), an increased developed surface area ( $S_{dr}$ ), and higher material volume on the peaks and in the valleys ( $V_{mp}$  and  $V_{vv}$ ).

- EtO and H<sub>2</sub>O<sub>2</sub> sterilisation methods damaged the electrospun mats. The UV sterilisation method maintained mat architecture and integrity and was thus used for the study.
- The wettability of the electrospun mats was not affected by texture or sterilisation.
- The absorption capacity of the mats did not vary between the sterile and non-sterile samples, proving the suitability of UV sterilisation for electrospun mats with an increased absorption capacity.
- The highest absorption rates were observed for the TC2 and TC4 textured mats. Absorption increased by 176.76% and 161.55%, respectively, after 1 h of use and by 58.25% and 46.4%, respectively, after 3 days of use, relative to the non-textured mats. A correlation between absorption capacity and hybrid surface parameters ( $S_{dq}$ ,  $S_{dr}$ ) was found.
- All mats proved to be biocompatible. Textured surfaces did not appear to have any effect on cell growth, likely due to the scale of the texture.

The present study demonstrates that absorption capability can be modulated with surface texture and identifies hybrid 3D areal parameters ( $S_{dr}$ ,  $S_{dq}$ ) as key surface characteristics for increased absorption. These findings serve as a foundation for the development of tailored surface textures designed to maximise exudation absorption in wound dressings. Future studies will focus on identifying optimum textures for generating ad-hoc textured collector plates using laser texturing.



**Acknowledgements**

This work was part of the ALOPRP3D project, which was funded by The Health Department of the Basque Government within the financial aid call for research projects and health development (refs.: 2020333032, 2021333057, 2022333044).

## References

1. Gefen A. How medical engineering has changed our understanding of chronic wounds and future prospects. *Medical Engineering and Physics*. 2019 October; 72: 13-18.
2. Sen CK. Human Wounds and Its Burden: An Updated Compendium of Estimates. *Advances in Wound Care*. 2019 February; 8(2): 39-48.
3. Mozafari M. Nanotechnology in Wound Care: One Step Closer to the Clinic. *Molecular Therapy*. 2018 September; 26(9): 2085-2086.
4. Janfada A, Asefnejad A, Khorasani MT, Joupari MD. Reinforcement of electrospun polycaprolacton scaffold using KIT-6 to improve mechanical and biological performance. *Polymer Testing*. 2020 April; 84.
5. MacEwan MR, MacEwan S, Kovacs TR, Batts J. What Makes the Optimal Wound Healing Material? A Review of Current Science and Introduction of a Synthetic Nanofabricated Wound Care Scaffold. *Cureus*. 2017 October; 9(10).
6. Saatchi A, Arani AR, Moghanian A, Mozafari M. Cerium-doped bioactive glass-loaded chitosan/polyethylene oxide nanofiber with elevated antibacterial properties as a potential wound dressing. *Ceramics International*. 2021 April; 47(7): 9447-9461.
7. Zarrintaj P, Moghaddam AS, Manouchehri S, Atoufi Z, Amiri A, Amirkhani MA, et al. Can regenerative medicine and nanotechnology combine to heal wounds? The search for the ideal wound dressing. *Nanomedicine*. 2017 October; 12(19): 2403-2422.
8. Mochane MJ, Motsoeneng TS, Sadiku ER, Mokhena TC, Sefadi JS. Morphology and

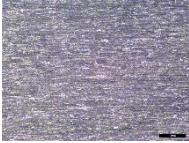
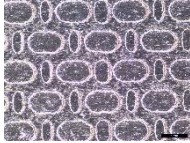
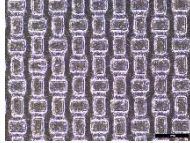


- Properties of Electrospun PCL and Its Composites for Medical Applications: A Mini Review. *Applied Sciences*. 2019 May; 9(11): 2205.
9. Cipitria A, Skelton A, Dargaville TR, Daltonac PD, Hutmacher DW. Design, fabrication and characterization of PCL electrospun scaffolds - A review. *Journal of Materials Chemistry*. 2011 June; 21(26): 9419-9453.
  10. Dhivya S, Padma VV, Santhini E. Wound dressings – a review. *Biomedicine*. 2015 December; 5(4): 22.
  11. Rad ZP, Mokhtari J, Abbasi M. Fabrication and characterization of PCL/zein/gum arabic electrospun nanocomposite scaffold for skin tissue engineering. *Materials Science and Engineering: C*. 2018 December; 93: 356-366.
  12. Redigueri CF, Sassonia RC, Dua K, Kikuchi IS, Pinto TdJA. Impact of sterilization methods on electrospun scaffolds for tissue engineering. *European Polymer Journal*. 2016 September; 82: 181-195.
  13. Griffin M, Naderi N, Kalaskar DM, Malins E, Becer R, Thornton CA, et al. Evaluation of Sterilisation Techniques for Regenerative Medicine Scaffolds Fabricated with Polyurethane Nonbiodegradable and Bioabsorbable Nanocomposite Materials. *International Journal of Biomaterials*. 2018 October.
  14. Dai Z, Ronholm J, Tian Y, Sethi B, Cao X. Sterilization techniques for biodegradable scaffolds in tissue engineering applications. *Journal of Tissue Engineering*. 2016 May; 7.
  15. Huang C, Thomas NL. Fabrication of porous fibers via electrospinning: strategies and

- applications. *Polymer Reviews*. 2020; 60(4): 595-647.
16. Simões D, Miguel SP, Correia IJ. Biofunctionalization of electrospun poly(caprolactone) fibers with Maillard reaction products for wound dressing applications. *Reactive and Functional Polymers*. 2018 October; 131: 191-202.
17. Li R, Cheng Z, Wen R, Zhao X, Yu X, Sun L, et al. Novel SA@Ca<sup>2+</sup>/RCSPs core-shell structure nanofibers by electrospinning for wound dressings. *RSC Advances*. 2018 April; 8(28): 15558-15566.
18. Yu H, Chen X, Cai J, Ye D, Wu Y, Fan L, et al. Novel porous three-dimensional nanofibrous scaffolds for accelerating wound healing. *Chemical Engineering Journal*. 2019 August; 369: 253-262.
19. Hejazi F, Mirzadeh H. Novel 3D scaffold with enhanced physical and cell response properties for bone tissue regeneration, fabricated by patterned electrospinning/electrospraying. *Journal of Materials Science: Materials in Medicine*. 2016 September; 27(9): 143.
20. Lin J, Ding B, Yang J, Yu J, Sun G. Subtle regulation of the micro- and nanostructures of electrospun polystyrene fibers and their application in oil absorption. *Nanoscale*. 2011 November; 4(1): 176-182.
21. Rogers CM, Morris GE, Gould TWA, Bail R, Toumpaniari S, Harrington H, et al. A novel technique for the production of electrospun scaffolds with tailored three-dimensional micro-patterns employing additive manufacturing. *Biofabrication*. 2014 September; 6(3).

22. Hosseini NS, Bölgen N, Khenoussi N, Yılmaz ŞN, Yetkin D, Hekmati AH, et al. Novel 3D electrospun polyamide scaffolds prepared by 3D printed collectors and their interaction with chondrocytes. *International Journal of Polymeric Materials and Polymeric Biomaterials*. 2017 July; 67(3): 143-150.
23. Grgurić TH, Mijović B, Zdraveva E, Bajsić EG, Slivac I, Ujčić M, et al. Electrospinning of PCL/CEFUROXIM® fibrous scaffolds on 3D printed collectors. *The Journal of The Textile Institute*. 2020 January; 111(9): 1288-1299.
24. Zdraveva E, Mijović B, Bajsić EG, Slivac I, Grgurić TH, Tomljenović A, et al. Electrospun PCL/cefuroxime scaffolds with custom tailored topography. *The Journal of Experimental Nanoscience*. 2019 June; 14(1): 41-55.
25. Tato W, Blunt L, Llavori I, Aginagalde A, Townsend A, Zabala A. Surface integrity of additive manufacturing parts: A comparison between optical topography measuring techniques. *Procedia CIRP*. 2020; 87: 403-408.
26. International Organization for Standardization (ISO). Geometrical product specifications (GPS) — Surface texture: Areal — Part 2: Terms, definitions and surface texture parameters. ; 2021.
27. Ghobeira R, Philips C, Naeyer VD, Declercq H, Cools P, Geyter ND, et al. Comparative Study of the Surface Properties and Cytocompatibility of Plasma-Treated Poly-ε-Caprolactone Nanofibers Subjected to Different Sterilization Methods. *The Journal of Biomedical Nanotechnology*. 2017 June; 13(6): 699-716.

28. Metavarayuth K, Sitasuwan P, Zhao X, Lin Y, Wang Q. The Influence of Surface Topographical Cues on the Differentiation of Mesenchymal Stem Cells In Vitro. *ACS Biomaterials Science and Engineering*. 2015 December; 2(2): 142-151.
29. Tudureanu R, Handrea-Dragan IM, Boca S, Botiz I. Insight and Recent Advances into the Role of Topography on the Cell Differentiation and Proliferation on Biopolymeric Surfaces. *International Journal of Molecular Sciences*. 2022 July; 23(14): 7731.
30. Chen M, Patra PK, Warner SB, Bhowmick S. Role of Fiber Diameter in Adhesion and Proliferation of NIH 3T3 Fibroblast on Electrospun Polycaprolactone Scaffolds. *Tissue Engineering*. 2007 March; 13(3): 579-587.

**Table 1.** Microscopic view of the textured collector plates and the corresponding  $S_a$  values  
(scale bars are 1 mm)

	CC	TC1	TC2	TC3	TC4
Photo					
$S_q$ ( $\mu\text{m}$ )	0.47	13.23	21.63	23.89	40.05

**Table 2.** Total number of cells counted LIVE and DEAD in each condition at 24, 48 and 72 hours

	24 h			48 h			72 h		
	N1	N2	N3	N1	N2	N3	N1	N2	N3
<b>LIVE</b>									
<b>CC</b>	186	232	189	174	219	388	437	214	325
<b>TC1</b>	136	-	211	269	86	226	214	241	284
<b>TC2</b>	45	93	286	350	289	170	591	-	209
<b>TC3</b>	-	194	433	62	59	353	280	281	357
<b>TC4</b>	151	187	356	817	399	198	156	390	442
<b>DEAD</b>									
<b>CC</b>	17	22	42	10	7	20	26	30	49
<b>TC1</b>	6	-	46	37	37	49	24	17	31
<b>TC2</b>	19	59	61	9	14	169	75	-	61
<b>TC3</b>	-	47	37	45	105	24	4	27	35
<b>TC4</b>	61	29	46	44	12	65	17	42	31



**Figure 1.** Axonometric projections of measurements carried out both on the textured collectors (CC, TC1, TC2, TC3, TC4) and on the mats electrospun on each one of them

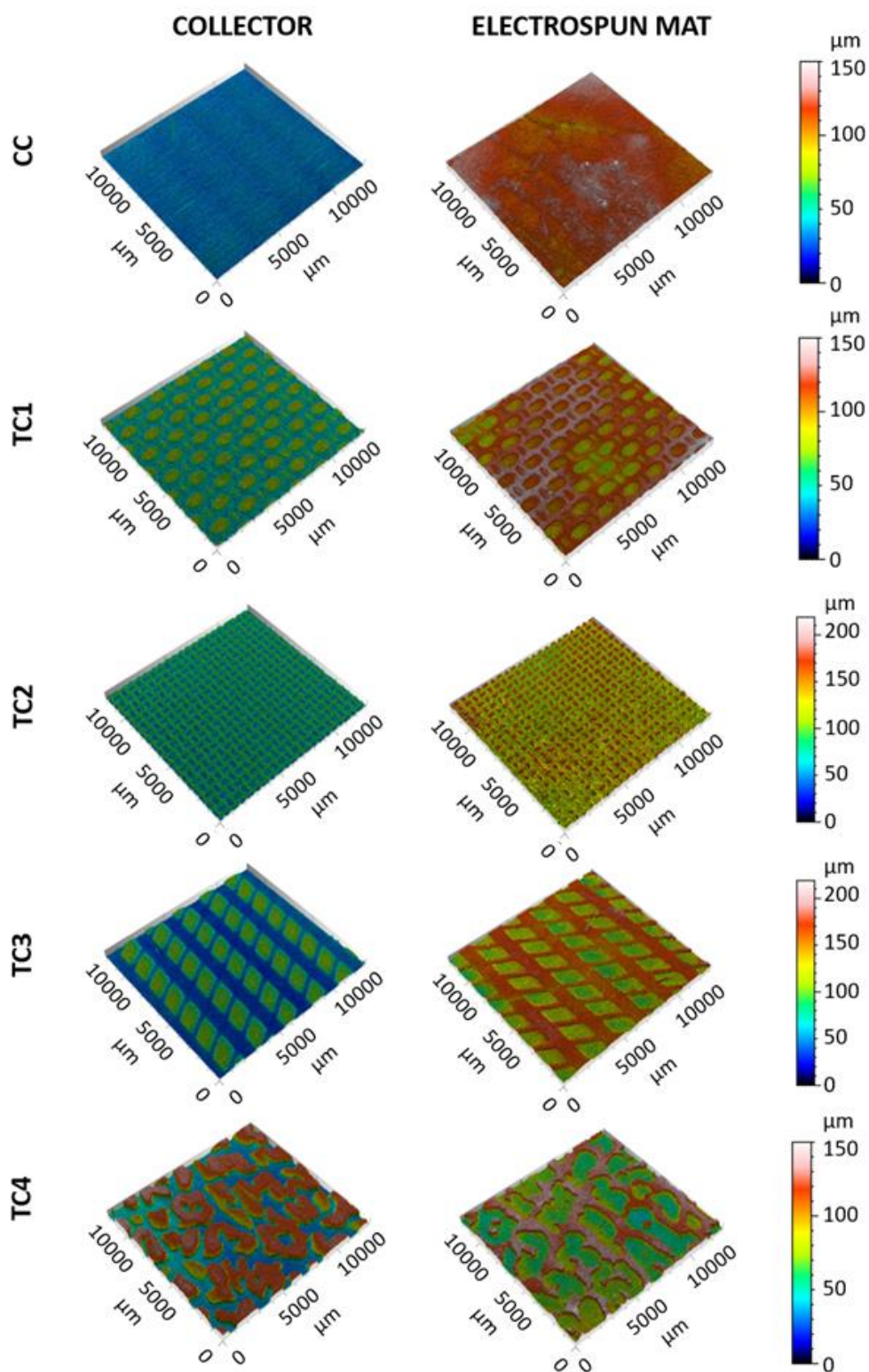


**Figure 2.** Topographic parameters corresponding to height ( $S_a$ ,  $S_{sk}$ ), hybrid ( $S_{dr}$ ,  $S_{dq}$ ) and functional ( $V_{mp}$ ,  $V_{vv}$ ) families of the collector-mat pairs of all collector types (CC, TC1, TC2, TC3, TC4) quantified via the optical profilometer

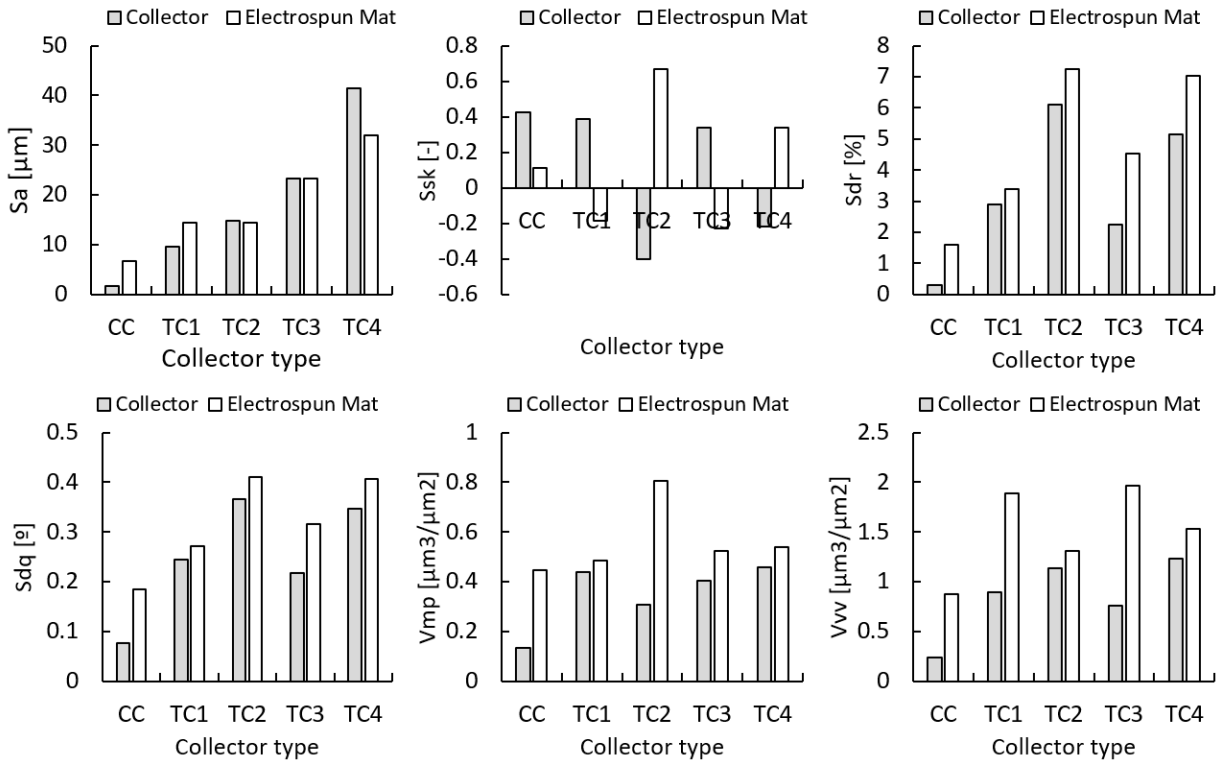


**Figure 3.** SEM images of electrospun mats corresponding to all collector types (CC, TC1, TC2, TC3, TC4) without sterilisation and after undergoing different sterilisation procedures (EtO, H<sub>2</sub>O<sub>2</sub>, UV)

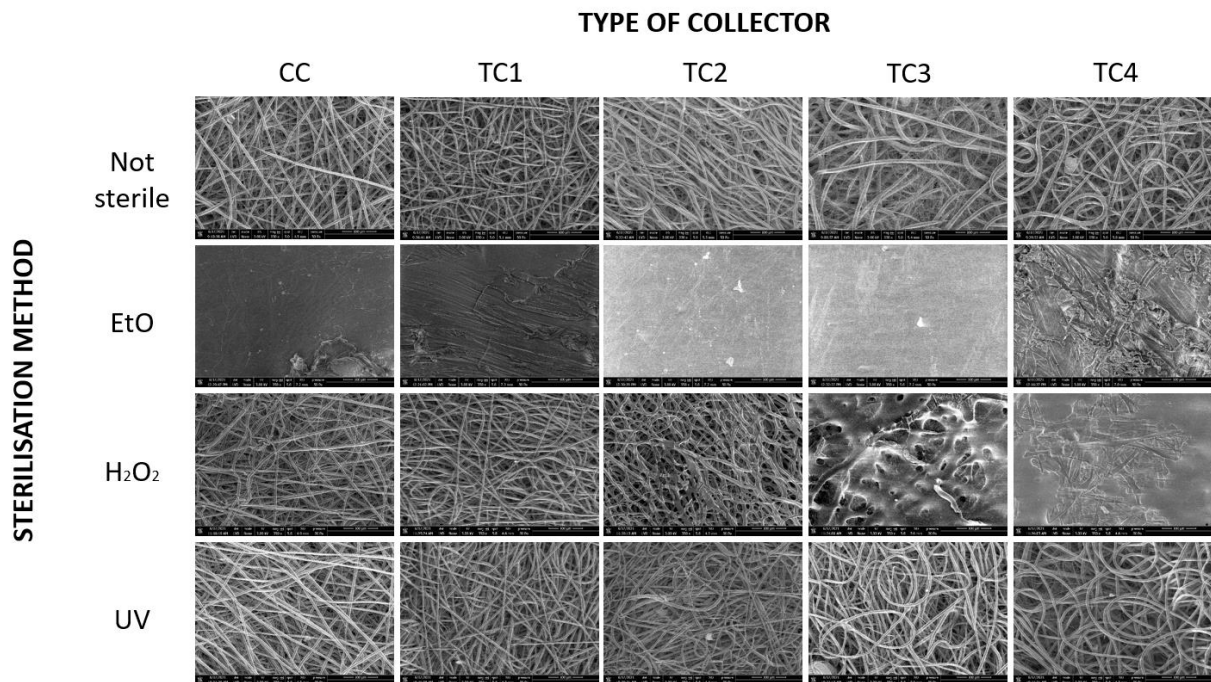


**Figure 4.** Fibre diameter values quantified for electrospun mats corresponding to all collector types (CC, TC1, TC2, TC3, TC4) for both non-sterilised samples (NS) and UV sterilised samples (UV)

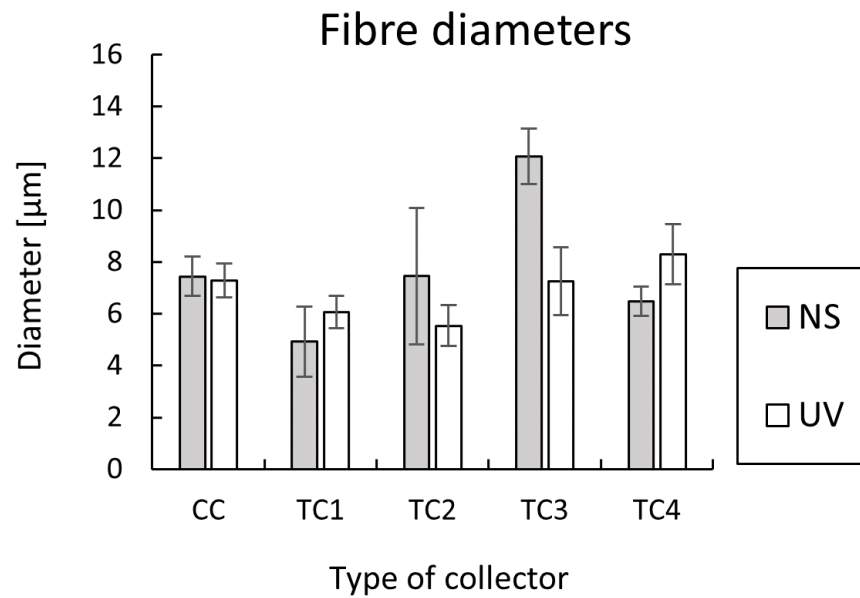


**Figure 5.** Contact angle values quantified for electrospun mats corresponding to all collector types (CC, TC1, TC2, TC3, TC4) for both non-sterilised samples (NS) and UV sterilised samples (UV)

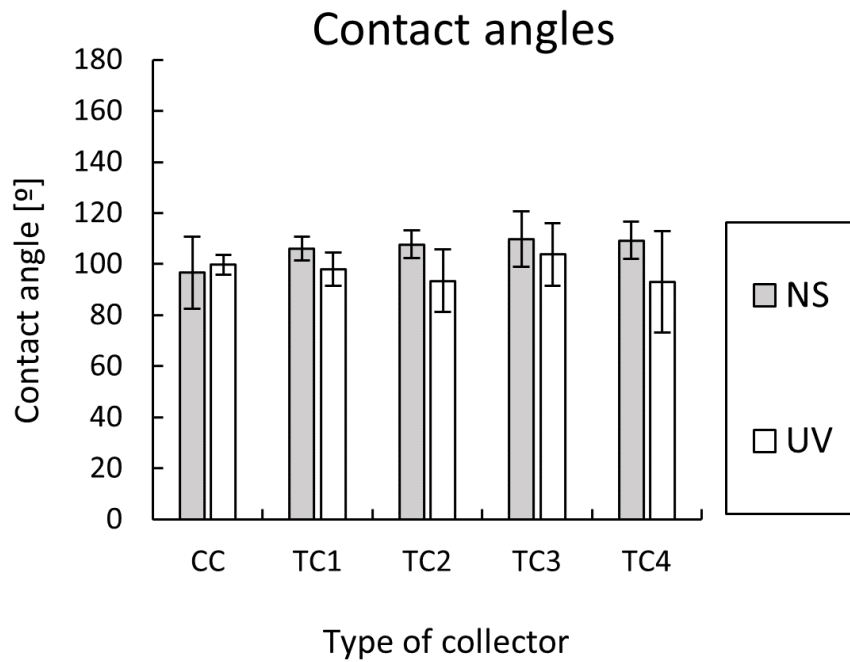


**Figure 6.** Absorption results for non-sterile and UV sterile electrospun mats corresponding to all collector types (CC, TC1, TC2, TC3, TC4) after immersion in HBSS for 1 h, 1 day, and 3 days

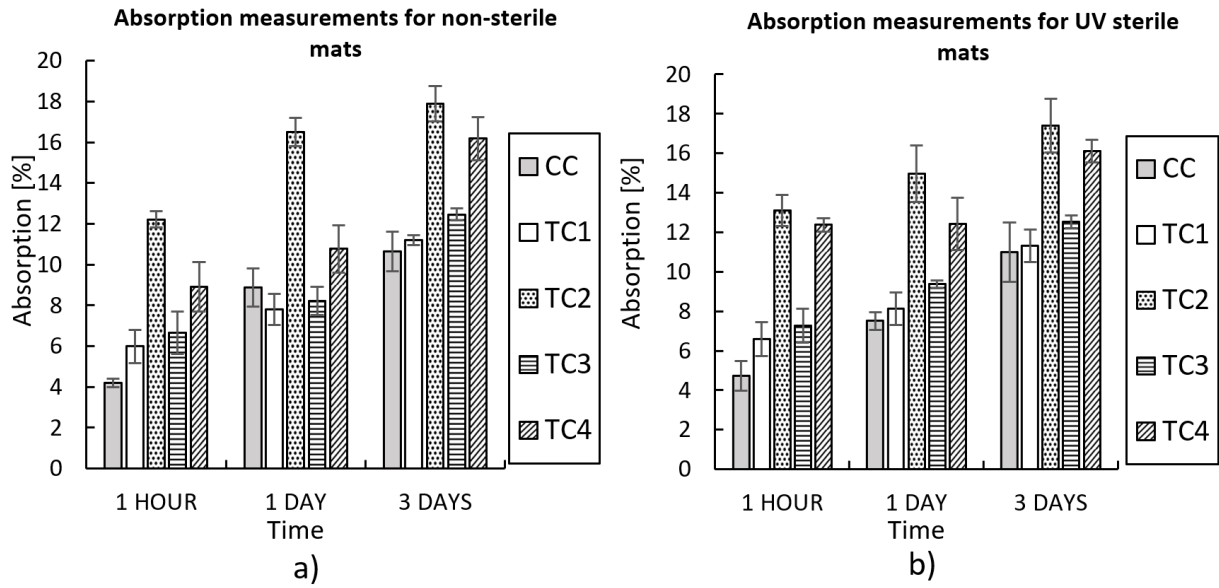


**Figure 7.** Height, hybrid and functional topographic parameters of all collector types (CC, TC1, TC2, TC3, TC4) plotted in descending order of absorption capability and normalised to the case that yields the highest absorption (TC2)

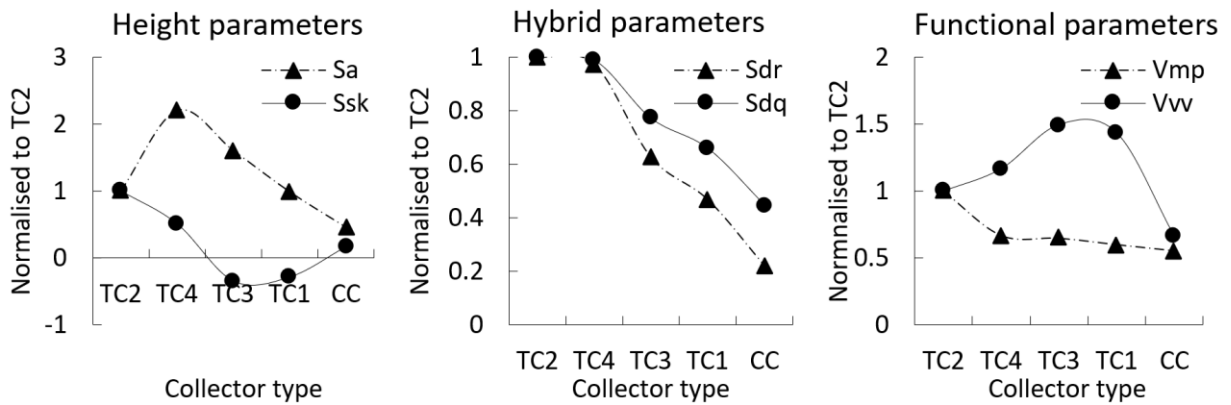
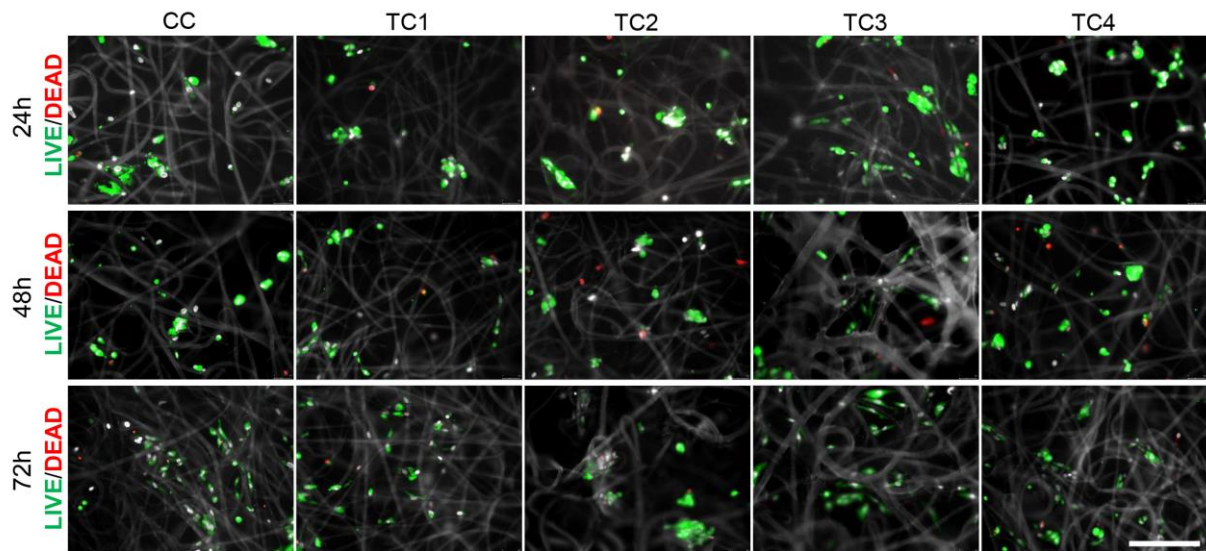
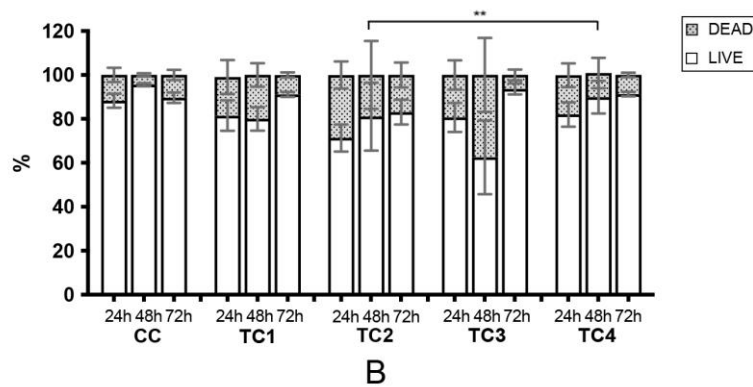


**Figure 8.** Cytotoxicity assays. A) Images of LIVE and DEAD cells in each culture condition at 24 h, 48 h and 72 h (LIVE cells are shown in green, and DEAD cells are shown in red). B) Percentage of LIVE and DEAD cells in each condition at 24 h, 48 h and 72 h



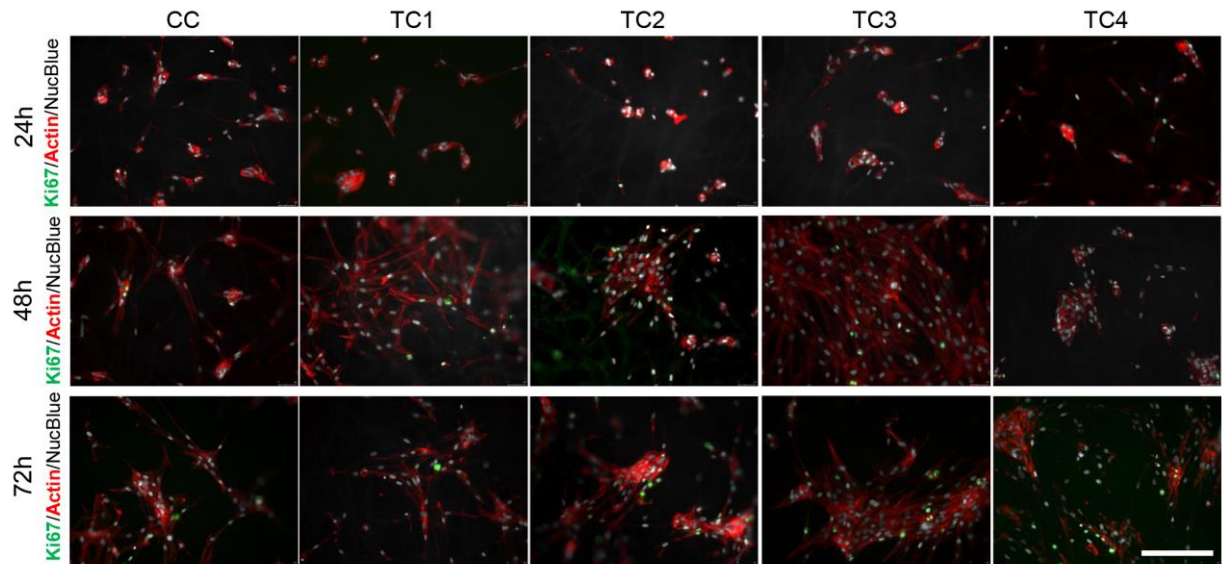
A



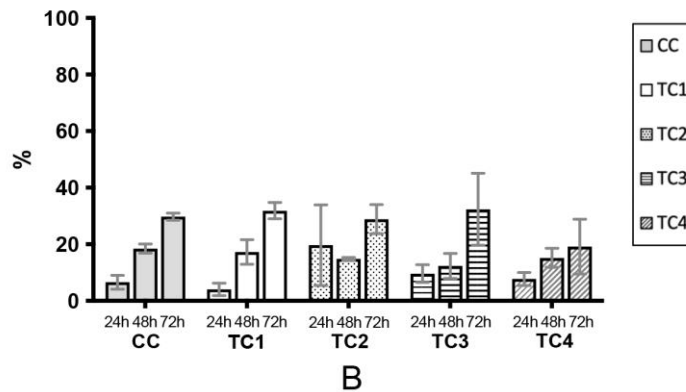
B



**Figure 9.** Proliferation assays. A) Immunofluorescence of fibroblasts in different culture conditions at 24 h, 48 h and 72 h (Ki67 expression in green and Actin expression in red). B) Percentage of proliferating cells in each condition at 24 h, 48 h and 72 h



A



B